Mon. Not. R. Astron. Soc. **000**, 000–000 (0000) Printed 22 April 2014 (MN LaTeX style file v2.2)

Modeling Gamma-Ray Burst-Associated Type Ic Supernovae: a Genetic Algorithm-Based Approach

H. Thankful Cromartie[1⋆]
1 *University of North Carolina at Chapel Hill Department of Physics and Astronomy*

22 April 2014

ABSTRACT

Long-duration gamma-ray bursts (GRBs) have been shown to be associated with Type Ic supernovae (SNe). However, most GRBs occur at sufficiently high redshift that if a SN is detected at all, it is detected only photometrically, and then at comparable brightness to the GRB's afterglow (at NIR through UV wavelengths). Consequently, GRB afterglow modeling efforts, at least of intermediate-redshift, long-duration GRBs, require a reliable SN model or template, (1) so the afterglow may be modeled without the results being contaminated by the SN, and (2) so the luminosity and temporal stretching of the SN may also be measured. Traditionally, low-redshift GRB-SN 1998bw (z = 0.0087) has served as this template, but it is only one event, and its temporal and spectral coverage is not complete. However, two other low-redshift GRB-SNe – 2006aj and 2010bh (z = 0.033 and 0.059, respectively) – have since been observed, and like 1998bw, have densely sampled light curves spanning many NIR, visible, and UV bands. Here we present a unified, albeit empirical, GRB-SN model, simultaneously fit to all three of these rich data sets, that may be used in future GRB afterglow and GRB-SN modeling efforts. This model may also be used to investigate if the temporal and broad spectral properties of GRB-SNe differ from traditional Type Ic SNe in significant, or subtle, ways.

Key words: gamma-ray burst, supernova, genetic algorithm, SN 1998bw, SN 2006aj, SN 2010bh

1 INTRODUCTION

Separately, GRBs and SNe are some of the Universe's most energetic events. GRBs are the brightest events ever seen[1], characterized by highly relativistic jets that are observed when beamed towards the Earth. Their enormous brightness means that GRBs can be observed very far away, providing a tool to probe environments of the early Universe. SNe are different beasts, distinguished by more isotropic radiation. GRB jet energy, when corrected for relativistic beaming, is comparable to SN kinetic energy.[2] It was not until the late 1990s that observational data provided evidence that these two enormously powerful events sometimes occur in tandem. In this case, the combined light curves resemble that of a typical GRB afterglow contaminated by a SN "bump" during the GRB's fading. In this study, the author presents a model fitted simultaneously to three of these GRB-SNe in pursuit of the following: 1) By creating a better GRB-SN template for use in future modeling efforts, we will be able to better infer underlying properties of GRBs and their environments. In this sense, SNe are contaminants of GRB afterglows; therefore, the ability to model the two events simultaneously will produce a more accurate description of each. 2) We wish to better infer the range of GRB-SN behavior in both temporal and flux spaces. Built into the model are two stretch factors, one in each of these domains, that facilitate a quantitative comparison between GRB-SNe. 3) The model's flexibility will facilitate the comparison of GRB-associated with non-GRB-associated Type Ic SNe, potentially indicating physical differences between the disparate events. This effort will be of particular importance to the Afterglow Modeling Project (AMP) (paper in prep; see also Trotter 2011). AMP is modeling GRB afterglows of interest observed since first detection in 1997. The result will be a catalog of fitted empirical model parameters describing extinction and absorption along the line of sight

⋆ The author would like to acknowledge the immense collaboration and support provided by her advisor, Dr. Dan Reichart, postdoctoral advisor, Dr. Adam Trotter, as well as *Galapagos* developer Andrew Foster.

[1] In terms of EM radiation per solid angle
[2] SN kinetic energy is generally $\sim 10^{51}$ erg, while total GRB kinetic energy is $\sim 10^{52}$ erg (Woosley & Bloom 2006).

to each GRB, as well as afterglow emission, SN properties, and the distribution of gas and varieties of dust present in GRB environments.

1.1 The Properties of Type Ic GRB-SNe

The nature of the physical processes driving GRB-SNe was initially highly contested. The now-canonical *collapsar* model, however, has been widely accepted (e.g. Woosley & Bloom 2006). GRBs have historically been divided into two groups: short-duration, which may occur on timescales of 10s of milliseconds, and long-duration bursts, which take as long as 100s of seconds. It is now thought that most long-duration GRBs are accompanied by SN events (Woosley & Bloom 2006). In order to understand the mechanism behind long-duration GRB-SNe, we will first explore the two events – GRBs and SNe – separately.

1.1.1 GRBs: The Collapsar Model

GRB events begin with the death of a very massive ($\gtrsim 25M_\odot$) star. As its core collapses into a black hole, which must be rotating rapidly, an accretion disk is formed. The accretion disk lives on a timescale similar to that of the collapse timescale of the inner part of the star, generally on the order of seconds. Creation of the GRB's signature relativistic jets is described magnetohydrodynamically. Baryonic material in the accretion disk is receiving large amounts of energy in very little time. Radiation is therefore absorbed and this material must move. It is very likely driven and shaped by magnetic fields that collimate and confine the jets, which move ultra-relativistically ($\Gamma \sim 100$). The jets shoot out blobs of material that become pancake-shaped, all of which have slightly different Γ values. This discrepancy results in internal shocks in the outflow, which constitute the GRB proper. These shocks emit ~90% of their light in the form of γ-rays. This results in a single, combined shock, which begins to sweep up material from the ISM. When the swept-up mass is equal to the ejecta mass within a factor of Γ, which occurs at a radius called r_{dec}, the ejecta decelerates, creating shocks and emitting light via synchrotron radiation. This process creates both forward and backward shocks. Forward shocks are not highly polarized, but backward shocks come again under the influence of the jet's ordered magnetic field, causing high polarization fractions. This process is evidenced by extremely high polarization – around 30% in the recent case of GRB 120308A (Mundell et al. 2013) – of the early afterglow. The reverse shock emission, when present, fades within minutes, but the forward shock emission can last hours to days. This light comes to us in the form of longer wavelengths – x-ray through radio – from shock-energized electrons which spiral around field lines, resulting in synchrotron radiation. If the accretion disk survives for a longer period of time, more energy can be delivered into the GRB jets, refreshing these shocks. The emitted light from GRBs is boosted by a factor of Γ^4, making the afterglow observable at great distances by relatively small telescopes. Two of these factors of Γ come from relativistic beaming of radiation, another comes from blueshifting of the jet along our line of sight, and the last comes from relativistic time dilation.

1.1.2 Type Ic SNe

Type Ic SNe are classified as such because they are spectroscopically different from Types Ia and Ib. No Hydrogen, and sometimes no Helium, is present in their spectra, as it has already been blown away from the star in the form of stellar winds. Instead of the canonical core-collapse supernova, in which stellar infall bounces off of the central neutron star and rebounds outwards, GRB-SNe result when the stellar material accretes and is blown outwards by lateral shocks driven by the GRB jets (Woosley & Bloom 2006). The ejected material is mildly relativistic ($\sim 0.1c$). GRB and SN events happen simultaneously, but SNe appear much later in the light curve of GRB afterglows because of their nonrelativistic nature.

1.2 The Canonical Type Ic SN Model

Early models have relied on the first well sampled GRB-SN event detected, SN 1998bw, as their basis in modeling GRB-SN light curves and spectra. In order to avoid bias towards a single event, the methodology presented in this work allows simultaneous fitting to multiple GRB-SNe. The result is a more versatile model capable of describing GRB-SNe more generally. The model was constructed using data from three nearby GRB-SNe: 1998bw associated with GRB 980425, 2006aj associated with GRB/X-Ray Flash (GRB/XRF) 060218, and 2010bh associated with GRB/XRF 100316 D. Each is well sampled both spectrally and temporally, was observed at high signal-to-noise, and does not suffer from significant contamination by its GRB counterpart. GRB-SNe are seen as contaminants of late-time GRB data; therefore, the model serves to account for any observed flux not associated with the GRB itself.

2 OBSERVATIONS

Contributions to observational data of the three SNe at hand are plentiful. Data taken between seconds after the bursts and 500 days are available from archived sources. More than 1200 data points in 21 different filter frequencies ranging from NIR to UV were used in fitting the model. This bulk of data is critical to the success of the model; however, data taken and processed in different ways by different scientists made it imperative to pay close attention in calibrating and using each data set. Calibration groups were constructed by hand, taking into consideration the photometric technique, filter, and telescope used in data collection. Because our model already includes Milky Way extinction and host galaxy contamination as parameters, data corrected for Milky Way extinction was uncorrected using a program constructed by the author that employs the Cardelli et al (1989) model. Where available, observations of the GRB-SNe host galaxies were included at an arbitrarily large time after the burst (i.e. 1000 days). All data before 1.5 days were removed from the dataset, as they are contaminated either by shock breakout of the SN or the GRB afterglow. Notably, data from the UNC GRB team's Panchromatic Robotic Optical Monitoring and Polarimetry Telescope (PROMPT) array at Chile's CTIO is included in the set, the photometry of which was carried out by Bufano et al. between 2010 and 2012 (see Reichart et al. 2005 for more information about PROMPT). An early-time model with its own spectral component will be added before publication, likely in the form of a power law describing the GRB afterglow contamination.

The following is a brief summary of data used, sorted by SN and author.

2.1 SN 1998bw

2.1.1 *McKenzie & Schaefer, 1999*

The authors gathered photometric data in B, V, and I bands with the Yale 1-meter telescope at the Cerro Tololo Inter-American Observatory in Chile. Observations range from 63 to 186 days after the burst.

2.1.2 *Clocchiatti et al., 2011*

Gathering U, B, V, R, and I-band data ranging from 2 to ∼500 days from Sollerman, Galama, and their own group, the authors transformed each data set to the CTIO system, yielding data that appeared to have been calibrated simultaneously. Sollerman et al. observed using the ESO 3.6 m telescope on La Silla and the VLT/UT1 on Paranal (Sollerman et al. 2000). Galama et al. used data from the 50-inch telescope at the Australian National University's (ANU) Mt. Stromlo Observatory (MSO), the 30-inch telescope at MSO, the 40-inch telescope at the ANU Siding Spring Observatory, the Anglo-Australian Telescope at the Anglo-Australian Observatory, the 3.5-m New Technology Telescope (NTT), and the 1.5-m Danish and the 0.9-m Dutch telescopes at the European Southern Observatory (Galama et al. 1998). Clocchiatti et al. used the 0.9-m telescope at CTIO.

2.1.3 *Patat et al., 2001*

Patat et al. provide NIR light curves for 1998bw between 22 and 65 days post-burst collected using ESO–La Silla.

2.2 SN 2006aj

2.2.1 *Mirabal et al., 2006*

Miribal et al. provided extinction-corrected photometric values. In order to begin fitting to the data, it was necessary to add that extinction back. Observations were taken in U, B, V, R, and I bands using several MDM telescopes between 2 and 27 days after the burst.

2.2.2 *Ferrero et al., 2006*

Data in B, V, R, and I-bands were collected from several telescopes (The Very Large Telescope, Liverpool Telescope, and Katzman Automatic Imaging Telescope) between 3 and 25 days post-burst.

2.2.3 *Kocevski et al., 2007*

The authors report values at NIR frequencies using PARITEL between 2 and 16 days. It is uncorrected for extinction; however, host subtraction necessitated adding the reported host fluxes back into the data.

2.2.4 *Sollerman et al., 2006*

The author's data, in U, V, and R bands, was taken between 3 and 49 days after the burst using the ESO–La Silla telescope.

2.2.5 *Cobb et al., 2006*

Cobb et al. provided data in the I and J NIR bands using the SMARTS 1.3-m telescope at CTIO between 5 and 30 days post-burst.

2.2.6 *Campana et al., 2006*

UVOT data ($UVOT_u$, $UVOT_b$, $UVOT_v$, UVW1, UVM2, and UVW2) was reported in units of flux and was converted to Janskies using bandwidths provided by Campana et al. The data spans between 1.5 and 35 days.

2.3 SN 2010bh

2.3.1 *Cano et al., 2011*

Data is gathered in B, V, R, I, i', and several Hubble Space Telescope Wide-Field Camera 3 (WFC3) filter wavelengths. Extinction-corrected data was uncorrected before implementing the observations in the fits. Additionally, because some data was transformed by Cano et al. from WFC3 filters to the Johnson-Morgan-Cousins (JMC) UBVRI filter set, a separate calibration group was created to separate this UBVRI from the non-Hubble UBVRI observations. The observations span from 2 to 137 days.

2.3.2 *Olivares et al., 2012*

Olivares et al. provided optical and NIR data in g', r', i', z', J, H and Ks bands using GROND between 12 hours and 80 days after the burst.

2.3.3 *Bufano et al., 2012*

The JMC observations were taken using both the Very Large Telescope with the FORS2 and X-Shooter instruments and UNC's PROMPT array. Ranging between 2.5 and 62 days post-burst, the data were only modified in order to shift the phase from the galaxy frame to the observer frame.

3 THE GRB-SN MODEL & FITS

The model presented in this work consists of parameters dictating both the temporal and spectral evolution of GRB-SNe. It will be broken into its three constituent parts: the spectral model, "meta" model (which describes how the spectrum evolves in time) and temporal model.

3.1 *Galapagos: the Darwinian approach to GRB Modeling*

Gamma-Ray Bursts and Supernovae require the implementation of a model with a large number of parameters. *Galapagos*, a piece of modeling software built by the UNC GRB Team, uses genetic algorithms that mimic Darwinian

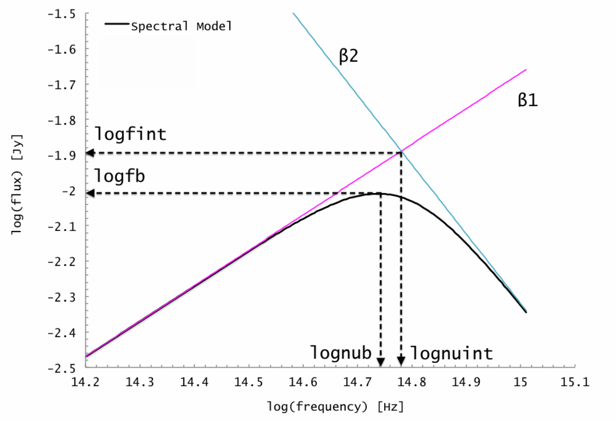

Figure 1. An example of the single-SBPL spectral model form.

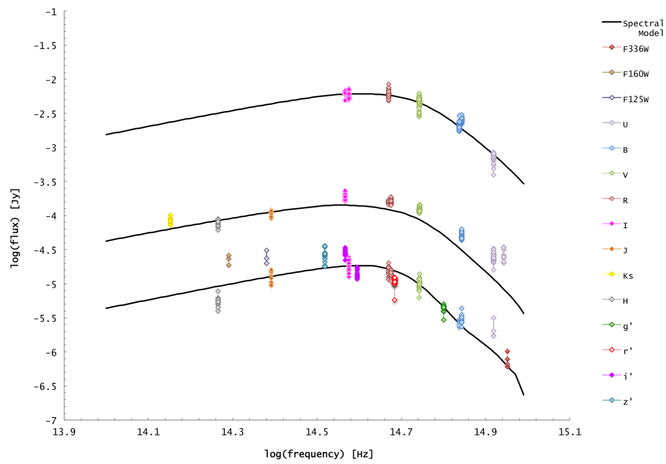

Figure 2. Spectral data for SNe 1998bw, 2006aj and 2010bh at log(t) = 1.5. Note the SBPL model fit to this data, as well as its correspondence to Figure 1.

evolution to combat getting stuck in local minima – a problem associated with large-dimensional models. Starting from user-defined parameter value ranges, *Galapagos* generates a random set of solutions and discards values that detract most from overall model fitness. Survivors are paired off and "offspring" are generated by random selection between their parameter values. After a number of generations (iterations), the model converges to the best fitness, a measure analogous to χ^2 in variance analysis. To avoid degeneracies and excess degrees of freedom, data gathered from prior analyses is used to constrain certain model parameters, especially those that dictate the shape of Galactic and host-galaxy extinction curves. When prior information is available, a Gaussian distribution centered on the expected parameter value is applied to each constrainable parameter; when the model takes on a high-sigma value, the fitness decreases. Additionally, *Galapagos* enables simultaneous fitting to temporally distinct data sets. It is therefore possible to link parameter values between GRB-SN events, meaning the user may specify whether a parameter should retain the same value regardless of the SN, or if it should be allowed freedom to change from burst to burst. As previously mentioned, a major impediment to GRB-SN modeling is differing photometry techniques that lead to constant offsets in light curves. *Galapagos* provides the user with the option of creating calibration offset groups that have the freedom to take on a constant flux density offset (albeit one that results in a larger hit to the model's overall fitness) in the interest of aligning with other calibration groups as though they had been reduced identically. This capability is critical in accounting for the discrepancies in archived data.

3.2 The Spectral Model

The behavior of the GRB-SNe's changing flux densities over frequency space can be modeled empirically with a smoothly-broken power law. The three spectral parameters to which we fit, β_1, the rising spectral slope, β_2, the falling spectral slope, and s, a smoothing parameter, are linked to be the same between SNe (see Figure 1). The break frequency of the smoothed curve is labeled *lognub*, while the break flux is *logfb*. We fit to the smoothed curve rather than the intersection of the two lines in order to prevent correlations between fitted parameter uncertainties. A plot (see Figure 2) is provided that displays real data from each of the three SNe and the corresponding fitted model. The equations governing this SBPL are as follows:

Table 1. Best-Fit Spectral Parameters

Parameter	SN1998bw	SN2006aj	SN2010bh	Linked?
beta1:	1.265	1.265	1.265	Yes
beta2:	-4.138	-4.138	-4.138	Yes
s:	-3.029	-3.029	-3.029	Yes

$$\log(\text{flux}) = l_1 + \frac{ln(e^{s\cdot(l_2-l_1)}+1)}{s}, \tag{1}$$

where the first line, l_1 is:

$$l_1 = logfint + \beta_1(lognu - lognuint) \tag{2}$$

and the second, l_2, is:

$$l_2 = logfint + \beta_2(lognu - lognuint) \tag{3}$$

The flux at the point of l_1 and l_2's intersection is related to *logfb* by:

$$logfint = logfb - \frac{1}{s}\cdot\ln[e^{\beta_1\cdot\frac{\ln\frac{-\beta_1}{\beta_2}}{\beta_2-\beta_1}} + e^{\beta_2\cdot\frac{\ln\frac{-\beta_1}{\beta_2}}{\beta_2-\beta_1}}] \tag{4}$$

Finally, the frequency at this intersection is related to *lognub* by:

$$lognuint = lognub - \frac{\ln\frac{-\beta_1}{\beta_2}}{s\cdot(\beta_2-\beta_1)} \tag{5}$$

Best-fit parameter values for the spectral model component can be found in Table 1.

3.3 The Meta Model

From an analysis of this spectral behavior, another SBPL was employed to describe the evolution of break frequency, *lognub*, over time. This "meta model" (see Figure 3) is defined by another five parameters: the break time *lognub_logtb*, break frequency *lognub_nutb*, initial and fi-

Table 2. Best-Fit Meta Parameters

Parameter	SN1998bw	SN2006aj	SN2010bh	Linked?
lognub_logtb:	1.530	1.530	1.530	Yes
lognub_nutb:	14.631	14.631	14.631	Yes
lognub_m1:	-0.291	-0.291	-0.291	Yes
lognub_m2:	0.033	0.033	0.033	Yes
lognub_s:	502.826	502.826	502.826	Yes

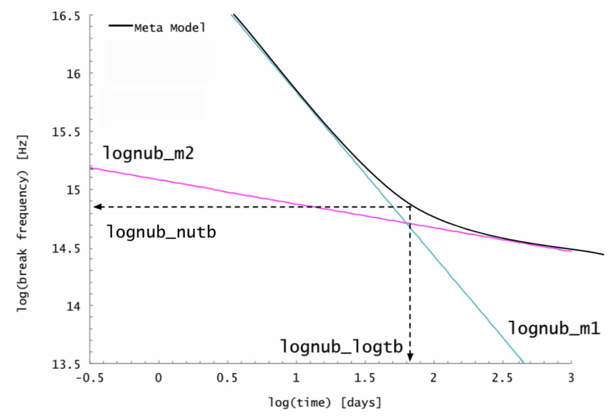

Figure 3. An example of the so-called SBPL "meta-model", which describes the evolution of break frequency over time.

nal slopes *lognub_m*1 and *lognub_m*2 and the smoothing parameter *lognub_s*. Like the spectral model, the meta-model is fit in log-log space using the equations presented in Section 3.2. Best-fit parameter values are found in Table 2.

3.4 The Temporal Model

The temporal model (see Figure 4) is motivated by Valenti et al. (2008), which models the behavior of non-GRB-associated Type Ic SNe. This work's temporal model is composed of two added smoothly broken exponential curves. Unlike the meta or spectral models, the temporal

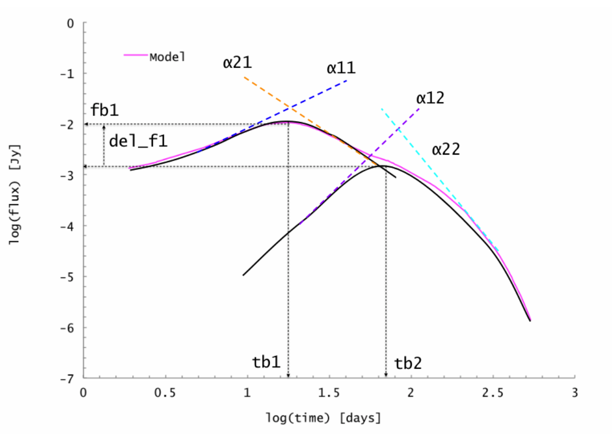

Figure 4. The temporal model, which is composed of two smoothly broken exponentials whose fluxes are added. Although defined in linear time, the plot shown above is in log(time) [days] in order to bring out temporal detail.

Table 3. Best-Fit Temporal Parameters

Parameter	SN1998bw	SN2006aj	SN2010bh	Linked?
tb1:	15.823	15.823	15.823	Yes
tb2:	71.600	71.600	71.600	Yes
Dtb:	0	-5.126	-7.233	No
fb1:	-1.878	-1.878	-1.878	Yes
alpha11:	0.237	0.132	1.666	No
alpha21:	-0.029	-0.029	-0.029	Yes
alpha12:	4.66E-08	4.66E-08	4.66E-08	Yes
alpha22:	-0.007	-0.007	-0.007	Yes
s1:	-0.762	-1.220	-0.102	No
s2:	-1189.340	-1189.340	-1189.340	Yes
del_f1:	-0.765	-0.687	-1.026	No
SF:	1.000	0.980	0.180	No
ST:	1.000	0.785	0.803	No

model is composed of smoothly broken exponentials; the functions are defined in linear, not log, time. The same scheme used to smoothly break two power laws is applied to the exponential functions, except the model uses linear time. The most important temporal model parameters are tb_1 and tb_2, the peak times of the two SBE curves, fb_1, the flux at the SN peak (the smoothed peak, not the intersection of the two "lines" that compose the SBE), del_f1, the offset in flux between the first and second SBPL peaks, α_{21}, the Nickel decay slope, and α_{22}, the late-time slope which is driven by Cobalt decay. The amount of time between tb_1 and tb_2 is constant, but the peaks are together allowed to shift in time relative to SN 1998bw (parameter *Dtb*). A stretching parameter, *ST*, applied around both tb_1 and tb_2, is built into the model to describe differences in SN evolution between bursts. An additional parameter, *SF*, is a shift in log flux (a stretch in linear flux) space that accounts for different SN luminosities. All SNe are shifted first into the source frame then into the rest frame of 1998bw to facilitate comparisons between the SNe. Best-fit temporal parameter values are found in Table 3.

Best-fit plots for SN 1998bw, SN 2006aj, and SN2010bh in 21 bands follow below. Data appear as black dots, and model fits as colored lines. Calibration offsets have been used in these fits, but are not plotted (the data have not been moved by any constant offset).

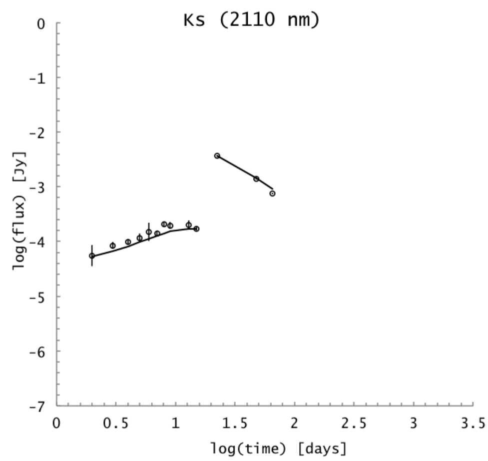

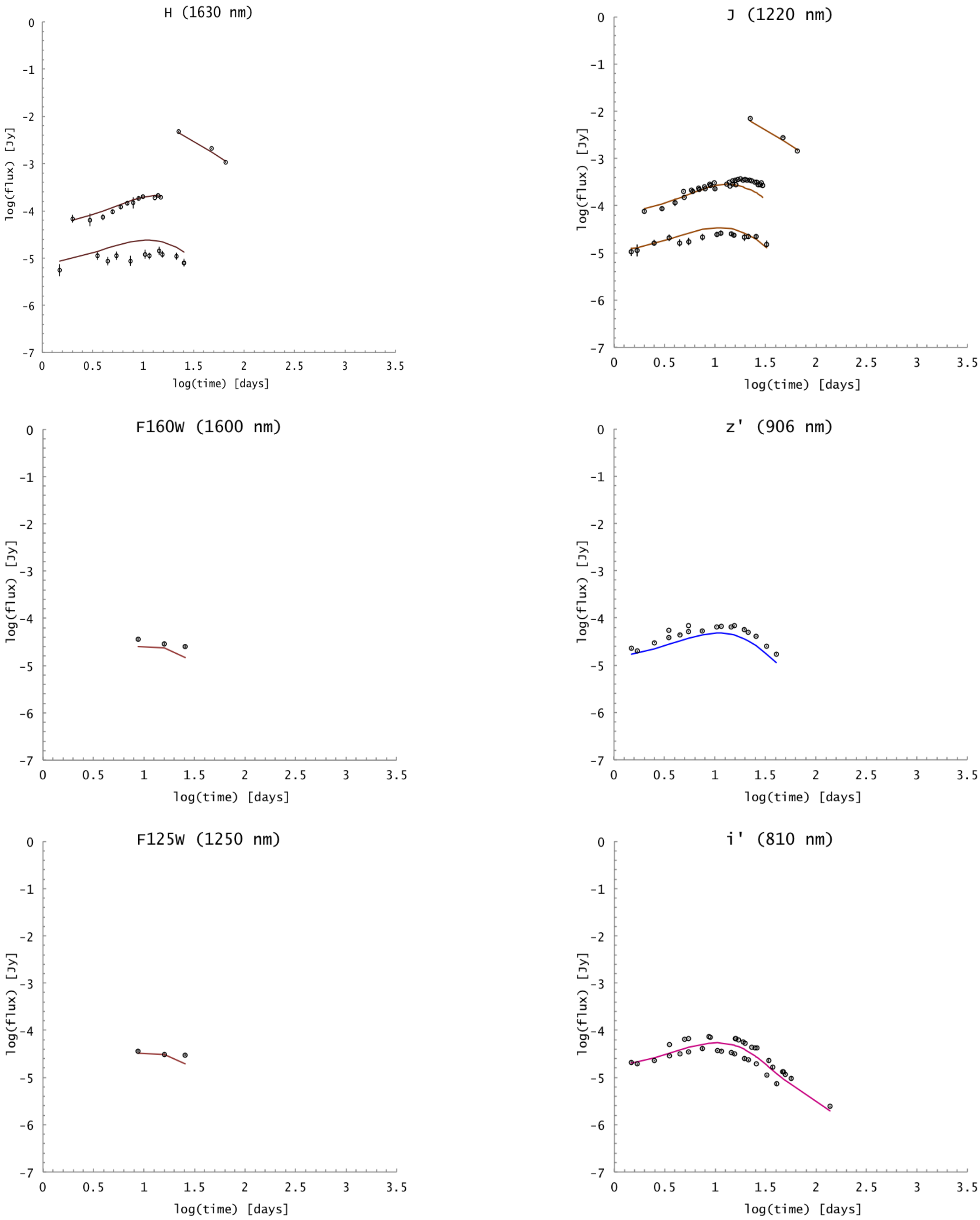
H (1630 nm)
J (1220 nm)
F160W (1600 nm)
z' (906 nm)
F125W (1250 nm)
i' (810 nm)
log(flux) [Jy]
log(time) [days]

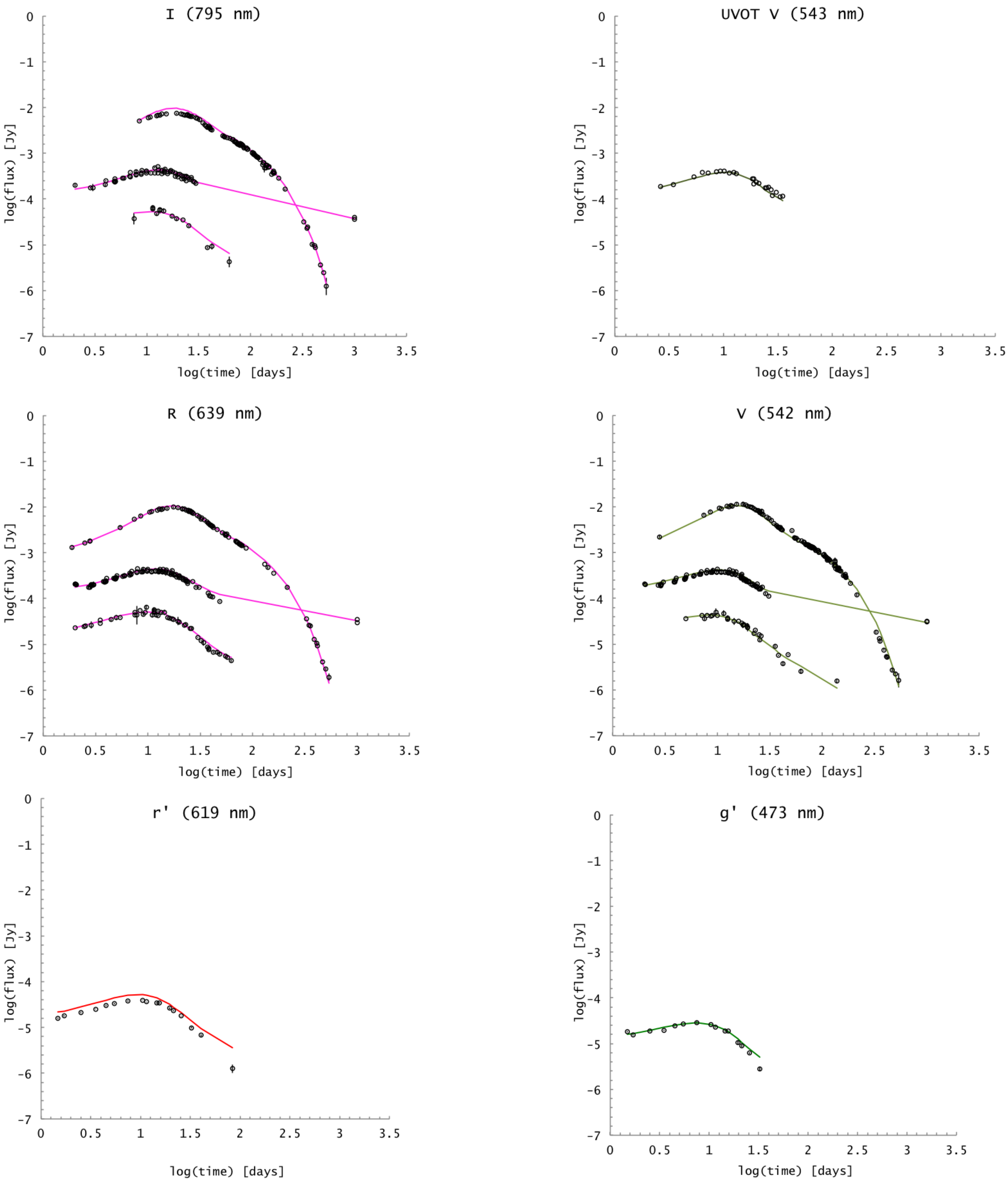
I (795 nm)
UVOT V (543 nm)
R (639 nm)
V (542 nm)
r' (619 nm)
g' (473 nm)
log(flux) [Jy]
log(time) [days]

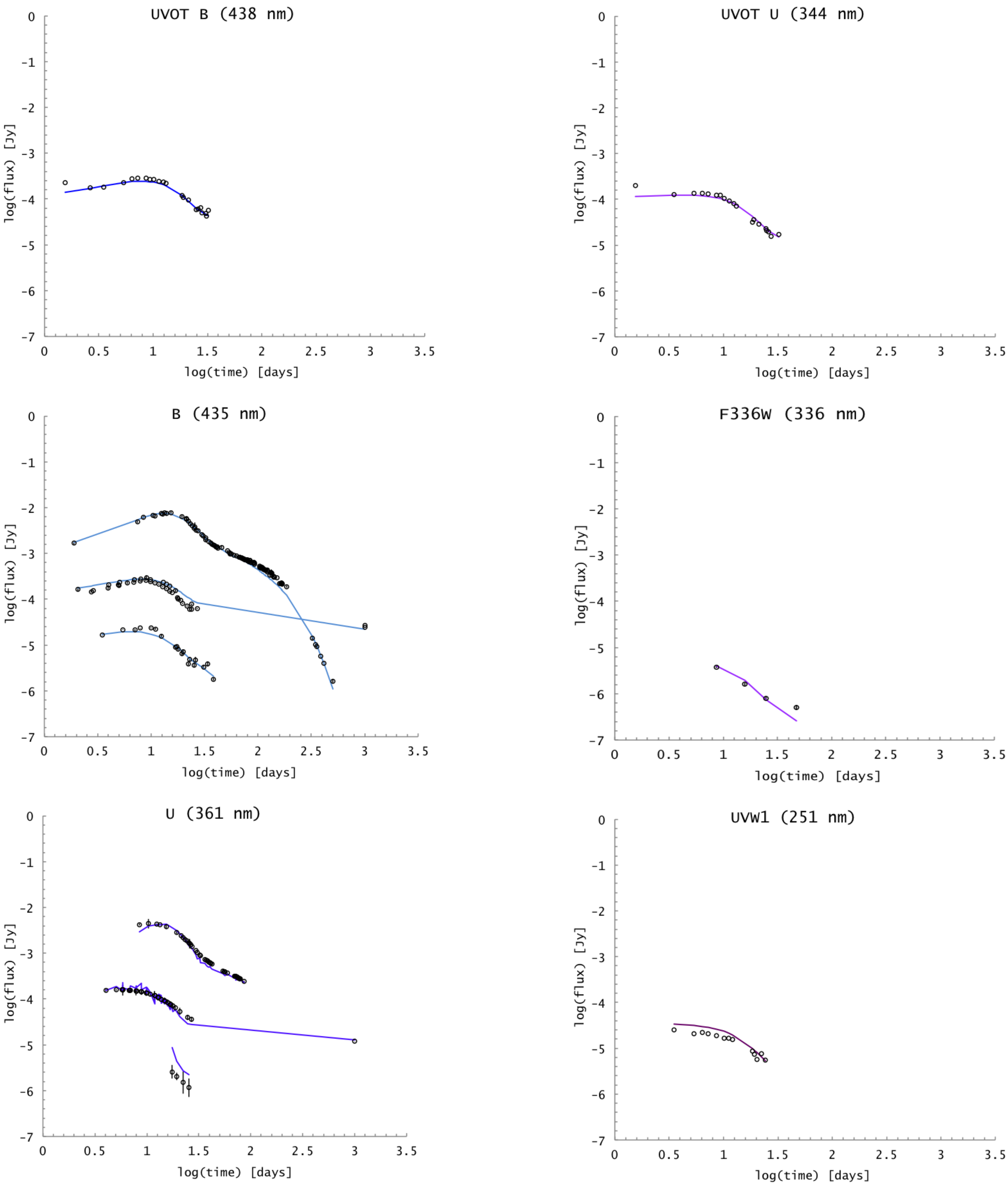
UVOT B (438 nm)
UVOT U (344 nm)
B (435 nm)
F336W (336 nm)
U (361 nm)
UVW1 (251 nm)
log(flux) [Jy]
log(time) [days]
0
-1
-2
-3
-4
-5
-6
-7
0.5
1
1.5
2
2.5
3
3.5

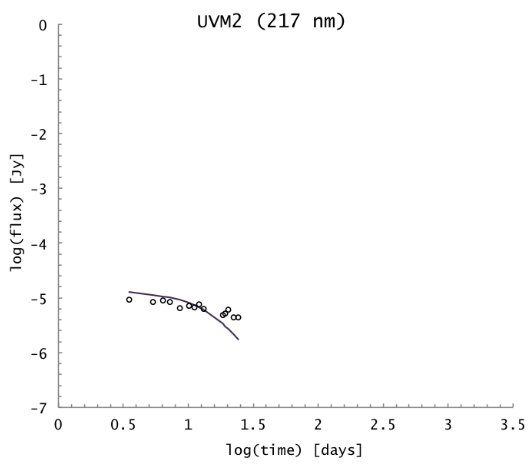

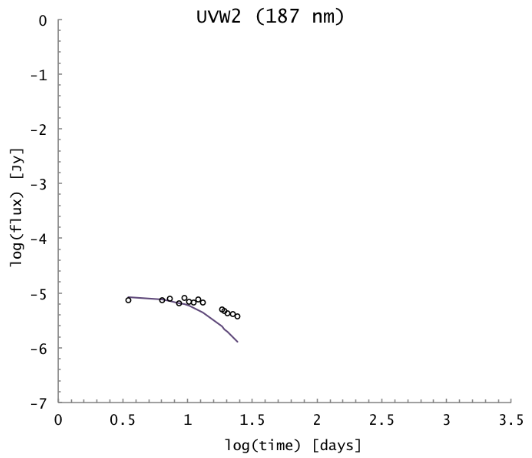

4 RESULTS & FUTURE WORK

We have created a very flexible model in temporal and spectral space to describe the SN component found in the afterglow curves of some GRB events. The model will prove to be helpful in accounting for SN contamination from GRB data, comparing GRB-SNe to each other, as well as comparing Type Ic GRB-associated SNe with those that are not associated with GRBs. In doing this final task, we will probe the fundamental differences between SNe occurring alongside GRBs and those that are seemingly disconnected from GRB outbursts. The next step will also include error bar fitting prior to submission to the Monthly Notices of the Royal Astronomical Society in Summer 2014.

REFERENCES

McKenzie, E., Schaefer, B., The Late-Time Light Curve of SN 1998bw Associated with GRB 980425, Publications of the Astronomical Society of the Pacific, 111.

Clocchiatti, A. et al., The Ultimate Light Curve of SN 1998bw/GRB 980425, The Astronomical Journal, 141.

Patat, F. et al., The Metamorphosis of SN 1998bw, ApJ, 555.

Mirabal, N. et al., GRB 060218/SN 2006aj: A Gamma-Ray Burst and Prompt Supernova at z = 0.0335, ApJ, 643.

Campana, S. et al., The shock break-out of GRB060218/SN2006aj, Nature, 442.

Cobb, B. et al., SN 2006aj and the nature of low-luminosity gamma-ray bursts, ApJ Letters, 645.

Ferrero, P. et al., The GRB 060218/SN 2006aj event in the context of other gamma-ray burst supernovae, Astronomy & Astrophysics, 457.

Kocevski, D. et al., Multicolor Infrared Observations of SN 2006aj. I. The Supernova Associated with XRF 060218, ApJ, 663.

Sollerman, J. et al., Supernova 2006aj and the associated X-Ray Flash 060218, Astronomy & Astrophysics, 454.

Cano, Z. et al., XRF 100316D/SN 2010bh and the Nature of Gamma-Ray Burst Supernovae, ApJ, 740.

F. Olivares E. et al., The fast evolution of SN 2010bh associated with XRF 100316D, Astronomy & Astrophysics, 539.

Bufano, F. et al., The Highly Energetic Expansion of SN 2010bh Associated with GRB 100316D, ApJ, 753.

Reichart, D. et al., PROMPT: Panchromatic Robotic Optical Monitoring and Polarimetry Telescopes, Nuovo Cimento, 28.

Cardelli, J. et al., The relationship between infrared, optical, and ultraviolet extinction, ApJ, 345.

Woosley, S. & Bloom, J., The Supernova – Gamma-Ray Burst Connection, Astronomy & Astrophysics, 44.

Valenti, S. et al., The broad-lined Type Ic supernova 2003jd, MNRAS, 383.

Galama, T. et al., An unusual supernova in the error box of the big gamma-ray burst of 25 April 1998, Nature, 395.

Trotter, A., The Gamma-Ray Burst Afterglow Modeling Project: Foundational Statistics and Absorption & Extinction Models, dissertation at UNC-Chapel Hill Dept. of Physics & Astronomy.

Sollerman, J. et al., SN 1998bw at Late Phases, ApJ, 537.

Mundell, C. et al., Highly polarized light from stable ordered magnetic fields in GRB 120308A, Nature, 504.